Corrosion Inhibition of 5-Methyl-2H-imidazol-4-carboxaldehyde and 1H-Indole-3-carboxyaldehyde on Mild Steel in 1.0 M HCl: Gravimetric Method and DFT Study.

B. Semire*, F. A. Adekunle, S. B. Akanji, V. Adewumi

Department of Pure and Applied Chemistry, Faculty of Pure and Applied sciences,
Ladoke Akintola University of Technology, Ogbomoso, Oyo State, Nigeria.
*Corresponding E-mail: bsemire@lautech.edu.ng: Phone: +2348038269809.

Abstract

Weight loss and Density Functional Theory (DFT) methods were used to study the corrosion inhibition of 5-methyl-2H-imidazol-4-carboxaldehyde and 1H-Indole-3-carboxaldehyde on mild steel in acid medium. The values of thermodynamic parameters such as free energy of adsorption (ΔG^{o}_{ads}), adsorption equilibrium constant (K_{ads}), adsorption entropy (ΔS^{o}_{ads}), adsorption enthalpy (ΔH^{o}_{ads}) and activation energy (E_a) were calculated and discussed. The adsorption process on mild steel surface showed that 4-methyl imidazol-5-carboxaldehyde and Indole-3-carboxaldehyde obey Freundlich and Temkin adsorption isotherms respectively. Density Functional Theory (DFT) calculations were carried out at B3LYP/6-31+G** level of theory in aqueous medium on the molecular structures to describe electronic parameters. The molecular parameters associated with inhibition efficiency such as E_{HOMO}, E_{LUMO}, band gap energy (E_{LUMO}- E_{HOMO}), softness (S), electron affinity (EA) and number of electrons transfer were calculated.

Keywords: 4-methyl imidazol-5-carboxaldehyde, Indole-3-carboxaldehyde, Weight loss, DFT

1.0 Introduction

Corrosion is one of the major problems facing industries that involve in the use of machine made from various metals, it causes hazard to the society as well as the human

population. Different methods such as galvanization, cathode protection and recently the use of organic compound as corrosion inhibitor has been suggested and implemented, to minimize the effect of corrosion on metals. Among the efficient corrosion inhibitors used to prevent deterioration of metals are heterocyclic organic compounds consisting of a π-electron system [1-3]. Most effective and efficient corrosion inhibitors are organic compounds with hetero atoms and functional groups, they are capable of facilitating the adsorption onto the metal surface [4]. Thereto, these heterocyclic organic compounds are very important in biological reaction, environmental friendly, easily synthesized and purified [5]. The effectiveness of these organic compounds as corrosion inhibitors has been interpreted in terms of their molecular structures, molecular size, molecular mass, presence of hetero-atoms, electron density at the donor atoms, aromaticity and adsorptive tendencies, the frontier molecular orbital; HOMO (higher occupied molecular orbital) energy, the LUMO (lower unoccupied molecular orbital) energy, chemical potential (μ) and hardness (η), electronegativity (χ), and electron transfer number (ΔN) among others [6-11].

The corrosion inhibition efficiency (IE) of organic compounds is connected with their adsorption properties. The effect of the adsorbed inhibitor is to protect the metal from the corrosive medium [5]. Various inhibition mechanisms have been considered regarding different situations created by changing various factors such as medium and inhibitor in the system .i.e. metal/acid medium/inhibitor [12-13]. Theoretical approaches are now becoming popular to explain the interactions between the inhibitor molecules and the metal surface, therefore recently a trend is the involvement of the theoretical methods in corrosion studies [14-16].

The adsorption of the inhibitor onto the metal surface proceeds through charge transfer from the charged inhibitor's molecule to the charged metal (physical adsorption) or by electron

transfer from the inhibitor molecule to the metal (chemical adsorption). In all cases, chemisorption succeeds physiosorption; therefore, corrosion inhibition process can be viewed as a process that involves electrophilic and nucleophilic attack [17-19]. Therefore, molecular reactivity descriptors as such global electrophilicity/nucleophilicity, global softness, local electrophilicity/nucleophilicity, local softness and molecular planarity have been observed to be very important parameters for an effective organic inhibitor. Planar molecules are adsorbed well on metal surface because more of the organic molecule (inhibitor) come in contact with the metal surface.

The aim of the present work is to study the inhibitive action of 5-methyl -2H-imidazol-4-carboxaldehyde and 1H-Indole-3-carboxaldehyde toward the corrosion of mild steel in 1.0M hydrochloric acid solution using weight loss and theoretical method (DFT). The effect of temperature on corrosion rate of mild steel and the inhibition efficiency of the studied molecules were investigated to compute some thermodynamic parameters necessary for the understanding of the corrosion mechanism.

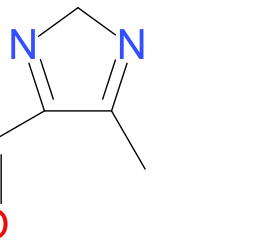

(a) 5-methyl-2H-imidazole-4-carbaldehyde

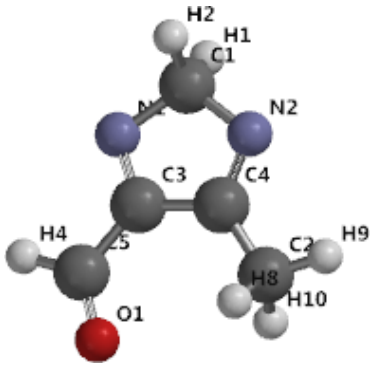

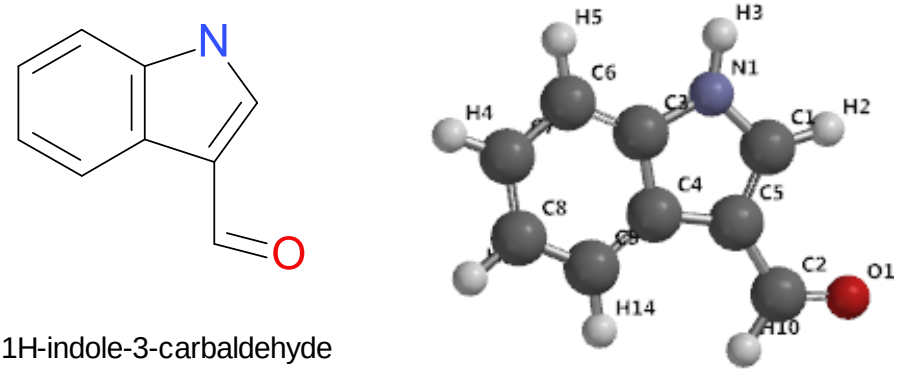

(b) 1H-indole-3-carbaldehyde

Figure 1: Schematic and Optimized structures of the studied inhibitors with numbering of atoms

2.0 Materials and methods

2.1 Experimental procedures

The carbon steel (containing 0.21% C, 0.35% Mn, 0.003% Si, 0.24% P and 99.20% Fe by mass) was mechanically press-cut into rectangular coupons of dimension 4.0 cm x 3.0 cm x 0.2 cm, grounded with SiC abrasive paper, degreased in ethanol, dried with acetone, weighed and stored in moisture free desiccators prior to usage [20]. The corrodent (acid) of 1.0M concentration was prepared from stock solution of HCl with 37% purity by serial dilution. The analytical grade (Sigma Aldrich) inhibitor (5-methyl-2H-imidazol-4-carboxaldeyhde and/or 1H-Indole-3-carboxyaldehyde) was added without further purification to the acid solution in concentration ranging from 1.0×10^{-4}µM, 0.8×10^{-4}µM, 0.6×10^{-4}µM, 0.4×10^{-4}µM and 0.2×10^{-4}µM in different beaker. The solution without inhibitor (blank) was taken as control experiment for comparison

The gravimetric measurements were conducted under total immersion in 50ml of test solution maintained at 303K-333K. The pre-cleaned and weighed carbon steel was immersed in beakers containing the test solutions, and weight loss was determined with respect to time. The coupon was retrieved from the test solutions at 1hour interval progressively for 5 hours and

immersed in 20% KOH solution, then removed and scrubbed, washed in distilled water, dried in acetone and weighed each time it been retrieved from the test solution [21].

The weight loss was taken to be the difference between the weight of coupon at a given time and its initial weight, using digital weighing balance with ± 0.001g sensitivity and the difference was used to compute the corrosion rate given by:

$\Delta W = W_1 - W_2$ which represent the weight loss.

The rate $(\rho) = \frac{\Delta w}{At}$ 1

where, W_1 = initial weight, W_2= weight after corrosion has occur, ΔW= change in weight.

The surface area covered by the inhibitor is given by:

Surface coverage $(\theta) = \frac{(\rho 1 - \rho 2)}{\rho 1}$ 2

while the efficiency of the inhibitor was calculated by:

Inhibition efficiency, $\% I.E = \left[\frac{\rho 1 - \rho 2}{\rho 1}\right] \times 100$ 3

where, ρ1 and ρ2 are rate of corrosion in the presence and absence of inhibitor respectively.

Thermodynamic parameters for the absorption process were observed from graph using Arrhenius equation (4) and transition state equation (5). Activation parameter for the corrosion process was thus calculated from the plotted graph [20,21].

$$\rho = A\, exp\left(\frac{-E_a}{RT}\right) \quad 4$$

$$\rho = \left(\frac{RT}{Nh}\right) exp\left(\frac{\Delta Sa^*}{R}\right) exp\ \frac{\Delta Ha^*}{RT} \quad 5$$

where (ρ) is the rate of corrosion for mild steel in 1.0M HCl solution, T is the absolute temperature, A is the Arrhenius factor/exponential factor, N is the Avogadro's number, R is the

universal gas constant, E_a is the activation energy for the corrosion process, ΔH_a^* is the enthalpy of activation, ΔS_a^* is the entropy of activation and h is the plank constant.

Three isotherms via Langmuir, Temkin and Freundlich were considered to determine the best fit isotherm for the corrosion inhibition of mild steel in 1.0M HCl.

2.2 Computational details

Conformational search was performed on 5-methyl-2H-imidazol-4-carboxaldehyde and 1H-Indole-3-carboxaldehyde employing semi-empirical AM1 method Monte Carlo search algorithm. For each conformational search, 1000 conformers were examined, only conformers within ±10 kJ/mol of energy window were considered. The lowest-energy conformer of this conformational search was taken for further DFT calculations [22]. All calculations were performed on the molecules with DFT of Becke's three parameter hybrid functional with correlation of Lee, Yang and Parr [23]. Optimization of molecules was performed at B3LYP/6-31+G** level of theory in gas phase [24]. Single point calculations were performed in aqueous medium at the same level of theory using optimized geometry obtained in the gas phase. The molecular descriptors calculated were chemical hardness (η), chemical softness (S), E_{HOMO} and E_{LUMO}, electronegativity (χ), electrophilicity index (ω), chemical potential (μ) and Fukui Function indices.

The conceptual DFT chemical potential is described as the first derivative of the energy with respect to the number of electrons in an external potential, which is equivalent to the negativity of the electronegativity (χ) [25,26].

$$\mu = \left(\frac{\partial E}{\partial N}\right) v(r) = -\chi = -\left(\frac{IP+EA}{2}\right) \approx -\left(\frac{E_{HOMO}+E_{LUMO}}{2}\right) \quad 6$$

where *E* is the total energy, μ is the chemical potential, *N* is the number of electrons, and $v_{(r)}$ is the external potential of the system.

Chemical hardness (η) is defined within the DFT concept as the second derivative of the energy (*E*) with respect to (*N*) as property which measures both stability and reactivity of the molecule [27,28] and softness as $\frac{1}{\eta}$.

$$\eta = \left(\frac{\partial^2 E}{\partial N^2}\right) v(r) = (IP - EA) \approx (E_{HOMO} - E_{LUMO}) \quad (7)$$

The number of electron transfer (ΔN) when two systems (i.e. Fe and inhibitor) are in contact is:

$$(\Delta N) = \frac{X_{Fe} - X_{inh}}{2(\eta_{Fe} + \eta_{inh})} \quad (8)$$

where X_{Fe} (taken to be 7.0eV) and X_{inh} are absolute electronegativity of the metal (Fe) and inhibitor molecule respectively, η_{Fe} (equals zero) and η_{inh} are the absolute hardness of Iron and the inhibitor molecule respectively.

The electrons flow from lower electronegative χ (inhibitor) to higher electronegative χ (Fe), until the chemical potentials becomes equal [28,29]. Fukui Functions was used to evaluate local reactivity indices as shown in equations 9 and 10;

$f^{+}_{(r)} = P_{N+1(r)} - P_{N(r)}$ (for nucleophilic attack) (9)

$f^{-}_{(r)} = P_{N(r)} - P_{N-1(r)}$ (for electrophilic attack) (10)

where $P_{N+1(r)}$, $P_{N(r)}$ and $P_{N-1(r)}$ are the electronic densities of anionic, neutral and cationic species respectively [29].

3.0 Result and discussion

3.1 Temperature on the rate of corrosion

The corrosion parameters such as weight loss (ΔW), corrosion rate (ρ), area coverage (θ) and inhibition efficiency (I.E) for mild steel in 1.0M HCl solution in the presence and absence of inhibitor with increase in temperature are shown in Table 1. Although, various factors influence the corrosion rate of metals, temperature has been considered as a principal factor that increases

the rate of corrosion and aggravates the deterioration of metal components [30,31]. Weight loss and corrosion rate increase with increasing temperature either in uninhibited system (blank) or inhibited system (either in the presence of 5-methyl-2H-imidazol-4-carboxaldehyde or 1H-Indole-3-carboxaldehyde) but decrease with increasing in inhibitor concentration at a particular temperature (Table 1).

Table1. Experimental data for the corrosion of mild steel in 1.0M HCl in the absence and presence of 5-methyl-2H-imidazol-4-carboxaldehyde (A) and 1H-Indole-3-carboxaldehyde (B)

Conc. / Temp.			Blank	2.0×10^{-5}	4.0×10^{-5}	6.0×10^{-5}	8.0×10^{-5}	1.0×10^{-4}
303K	ΔW	A	0.054	0.036	0.033	0.029	0.026	0.020
		B		0.019	0.018	0.017	0.016	0.013
	$P \times 10^{-5}$	A	4.590	3.060	2.750	2.522	2.253	1.701
		B		3.051	2.922	2.811	2.621	2.023
	Θ	A	-	0.333	0.401	0.451	0.509	0.630
		B	-	0.341	0.363	0.391	0.431	0.515
	I.E%	A	-	33.33	40.09	45.10	50.98	62.96
		B	-	34.10	36.32	39.12	43.10	51.51
313K	ΔW	A	0.073	0.059	0.052	0.046	0.043	0.036
		B		0.038	0.037	0.032	0.030	0.026
	$P \times 10^{-5}$	A	6.210	4.912	4.354	3.971	3.602	3.041
		B		4.845	4.583	4.122	3.841	3.460
	Θ	A	-	0.209	0.299	0.361	0.420	0.510
		B	-	0.223	0.262	0.342	0.384	0.443
	I.E%	A	-	20.93	29.95	36.07	42.02	51.04
		B	-	22.33	26.24	34.21	38.43	44.31
323K	ΔW	A	0.103	0.088	0.081	0.077	0.069	0.062
		B		0.071	0.068	0.063	0.058	0.052
	$P \times 10^{-5}$	A	8.501	7.404	6.890	6.382	5.870	5.271
		B		7.313	6.972	6.463	5.953	5.361
	Θ	A	-	0.129	0.189	0.249	*0.310*	0.380
		B	-	0.142	0.181	0.238	0.295	0.365
	I.E%	A	-	12.94	18.94	24.93	31.00	38.01
		B	-	14.21	18.10	23.81	29.52	36.51
333K	ΔW	A	0.136	0.131	0.131	0.121	0.113	0.104
		B		0.110	0.116	0.120	0.124	0.126
	$P \times 10^{-5}$	A	11.601	10.913	10.441	10.092	9.631	8.934
		B		10.861	10.482	10.263	9.658	9.165

	Θ	A B	- -	0.060 0.049	0.102 0.099	0.130 0.113	0.170 0.161	0.230 0.2085
	I.E%	A B	- -	6.04 4.90	10.20 9.90	13.02 11.32	16.98 16.13	23.02 20.85

The inhibition efficiency at a particular concentration decreases with increasing temperature which was due to desorption of inhibitor from metal surface which is associated with increase in temperature. As the temperature increases, the rate of corrosion of metal surface also increases. The rate of corrosion of iron in the presence of 1H-Indole-3-carboxaldehyde (B) is slightly higher than the rate of corrosion in the presence of 5-methyl-2H-imidazol-4-carboxaldehyde (A) at a particular concentration. For instance, at 6.0×10^{-5}M concentration of inhibitor, the rates of corrosion at 303K are 2.52×10^{-5} and 2.81×10^{-5}gcm^{-2}min^{-1} and at 333 K the corrosion rates are 10.09×10^{-5} and 10.26×10^{-5} gcm^{-2}min^{-1}for A and B respectively (Table 1). This suggests that 5-methyl-2H-imidazol-4-carboxaldehyde (A) is better corrosion inhibitor due to the presence of higher number of nitrogen atoms [32] which leads better adsorption of A on metal surface by interaction between the lone pairs of electrons of inhibitor nitrogen atoms and the metal surface [33].

3.2 The effect of concentration on the rate of corrosion.

Important information about the interaction between the inhibitor and steel surface can be provided by the adsorption isotherm. In this work, it can be concluded that surface coverage (θ) increases with the inhibitor concentration; this is attributed to more adsorption of inhibitor molecules onto the steel surface [34]. The corrosion rate (gcm^{-2}min^{-1}) depends on the concentration of inhibitor (5-methyl-2H-imidazol-4-carboxaldehyde and 1H-Indole-3-carboxyaldehyde) in 1.0M HCl acid solution at 303K-333K as shown in Table 1. The corrosion rate of the mild steel in the acid solution decreases with increasing concentration of the inhibitor,

this suggests that 5-methyl-2H-imidazol-4-carboxaldehyde and 1H-Indole-3-carboxaldehyde can be used as corrosion inhibitors for mild steel in 1.0M HCl acid solution. For instance, at 303K it is observed that the rate of corrosion decreases appreciably from 3.06×10^{-5} to 1.70×10^{-5} and 3.05×10^{-5} to 2.02×10^{-5} $gcm^{-2}min^{-1}$ for inhibitors A and B respectively as concentration increases from 0.2×10^{-4} to 1.0×10^{-4}M for inhibitor A.

It is well known fact that concentration of the inhibitor effect the rate of corrosion by increasing the surface coverage area of the inhibitor as the concentration increases [35]. At specific temperature, the surface coverage of the inhibitors on metal surface increases with increasing concentration of the inhibitor in both system (A and B), however larger surface coverage is observed with inhibitor (A) due to higher number of nitrogen atoms which leads better adsorption of A on metal surface by interaction between the lone pairs of electrons of inhibitor nitrogen atoms and the metal surface [32,33]. For instance, the surface coverage (θ) for A is 0.333, 0.401, 0.451, 0.509 and 0.630 at 303K, whereas it is 0.341, 0.363, 0.391, 0.431 and 0.515 for B at 303K with 0.2×10^{-4}M, 0.4×10^{-4}M, 0.6×10^{-4}M, 0.8×10^{-4}M and 1.0×10^{-4}M inhibitor's concentration respectively.

3.3 Thermodynamic activation parameters

Activation parameter for the corrosion process was calculated from Arrhenius equation (4) and transition state equation (5). The activation energy (E_a) for blank and optimum concentration of 5-methyl-2H-imidazol-4-carboxaldehyde and 1H-Indole-3-carboxaldehyde were determined from Arrhenius plot. Figures 1 shows that the linear regression coefficient for each molecule is close to one, implying that mild steel corrosion in 1.0M HCl can be studied using kinetic model.

The E_a values for the corrosion of the metal in the solution that contains the inhibitor is higher compared to that the uninhibited system (blank) as shown in Table 2. The E_a calculated for corrosion of iron in acidic solution containing 5-methyl-2H-imidazol-4-carboxaldehyde and 1H-Indole-3-carboxaldehyde as inhibitors are 45.943 and 39.117 kJ/mol respectively compared to 25.732 kJ/mol for the blank. This implies that adsorption occurred on the metal surface for the inhibited system (optimum concentration was used) and also show that 5-methyl-2H-imidazol-4-carboxaldehyde (A) is a better corrosion inhibitor.

ΔS_a^* and ΔH_a^* were calculated from equation 5, the plot of Ln(ρ/T) against 1/T shows a linear graph with $\Delta H_a^*/R$ as slope, and Ln(R/*Nh*) + $\Delta S_a^*/R$ as intercept. The enthalpy and entropy were evaluated for blank and optimum concentration from the plot. ΔH_a^* and ΔS_a^* for the dissolution reaction in the presence of inhibitor are higher than that in the absence of inhibitor (blank) (Table 2). The ΔH_a^* calculated for the dissolution reaction are 43.324, 26.986 and 23.113 kJ/mol for inhibitor A, inhibitor B and blank respectively. The positive sign for ΔH_a^* reflects the endothermic nature of the steel dissolution process, suggesting that the dissolution of mild steel is slow in the presence of inhibitor. The higher ΔH_a^* value for inhibitor A shows that more energy is required for corrosion to occur in the presence of 5-methyl-2H-imidazol-4-carboxaldehyde than in 1H-Indole-3-carboxaldehyde, this implies that corrosion occurs more slowly in the presence of inhibitor A; enhance better inhibition efficiency. The large negative value of ΔS_a^* implies that the activated complex is the rate determining step, rather than the dissociation step. The value of ΔS increases in the presence of inhibitor (Table 2), suggesting that there is an increase in the disorderliness as the reactants are converted into the activated complexes [30].

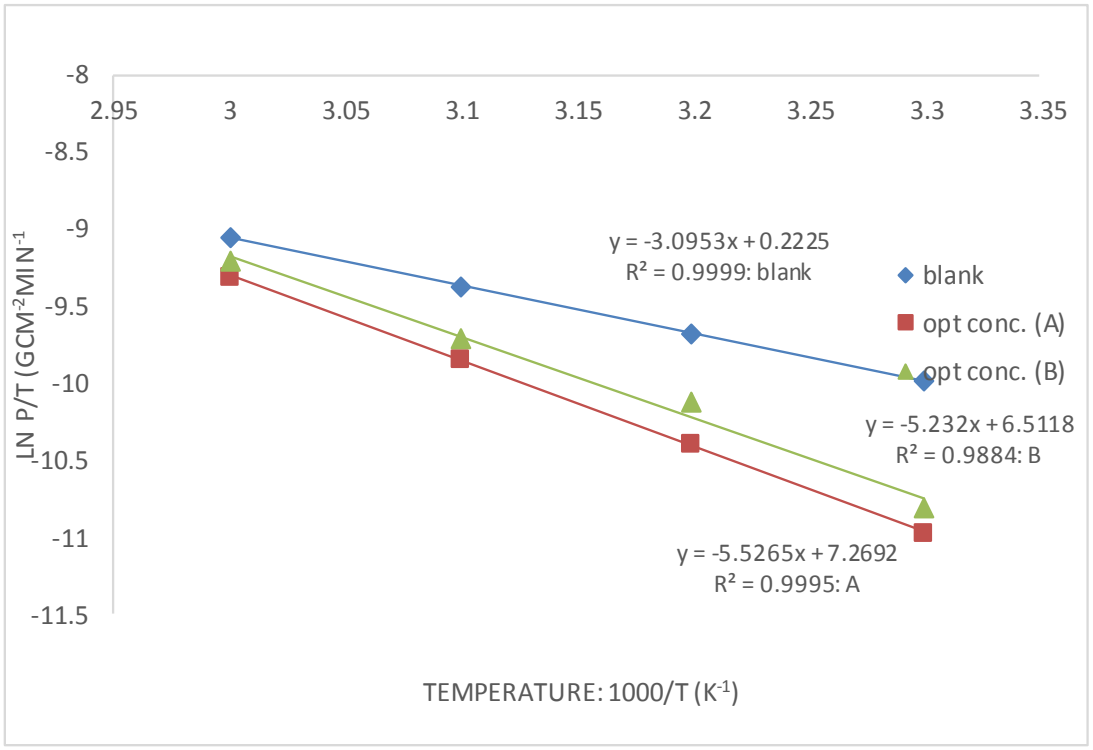

Figure 1. Graph of Ln (ρ/T) against 1000/T (K) at blank and optimum concentration for A and B

Table 2. Activation parameters for mild steel in 1.0M HCl solution for blank and optimum concentration of inhibitors A and B.

Inhibitor concentration		Corrosion Rate	R^2	E_a (kJ/mol)	ΔS_a^* (kJ/mol)	ΔH_a^* (kJ/mol)
Blank		4.59×10^{-5}	0.999	25.732	-251.834	23.113
1.0×10^{-4}M	A	1.70×10^{-5}	0.999	45.943	-193.258	43.324
	B	2.20×10^{-5}	0.988	39.117	-234.000	26.986

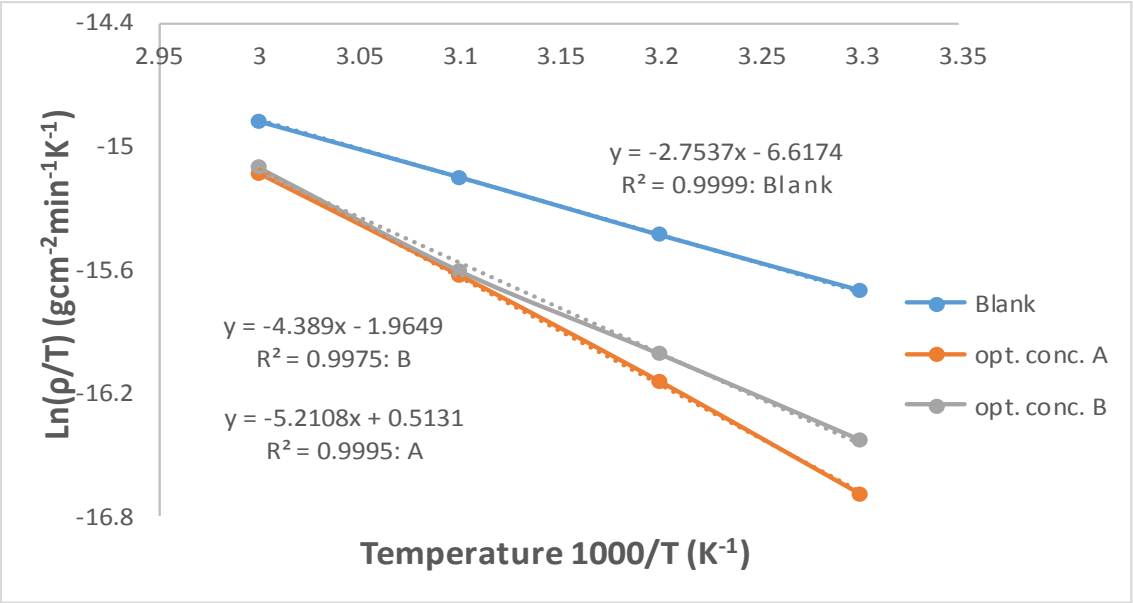

Figure 2. Transition state graph of Ln (ρ/T) against 1/T for blank and optimum concentration for A and B

3.4 Adsorption isotherms and thermodynamic parameters

Basic information on the interaction between the inhibitor and the metal surface can be provided by the adsorption isotherm, which depends on the degree of electrode surface coverage, θ [34]. A good organic inhibitor molecule tends to accept electron(s) from the d-orbital shell of the metal, and also donate electron(s) to the d-orbital shell of the metal thereby creating a system of forward and backward reaction called feedback reaction [3, 30, 33] until a quasi-equilibrium state is established. Therefore, it is reasonable to consider the quasi-equilibrium adsorption using the appropriate equilibrium isotherms. In this paper, three different isotherms were considered via Langmuir, Temkin and Freundlich isotherms to understand the adsorption process. The isotherm with the lowest adsorption constant (K_{ads}) and highest regression value is taken as the best fit isotherm for the adsorption process.

The estimated K_{ads}, slope and R^2 values for Langmuir, Freundlich and Temkin adsorption isotherms are listed in Table 2 as well as the free energy (ΔG_{ads}) values for the isothermic adsorption processes derived from equation 11:

$$\Delta G_{ads} = -R\,T\,ln\,(55.5\,K_{ads}) \qquad 11$$

where R is the universal gas constant, T is the thermodynamic temperature and the value of 55.5 is the concentration of water in the solution. The negative value calculated for ΔG_{ads} indicates spontaneous adsorption of the inhibitor onto the mild steel surface as well as the strong interaction between the inhibitor molecule and the metal surface [36,37].

Table 3. Thermodynamic parameters for the adsorption of 5-methyl-2H-imidazol-4-carboxaldehyde (A) and 1H-Indole-3-carboxaldehyde (B) in 1.0M HCl acid solution

Isotherms		Regression coefficient (R^2)	Free energy (ΔG_{ads} in kJ/mol)	K_{ads} (M^{-1})	Slope
Langmuir	A	0.921	-37.374	50000	1.593
	B	0.936	-35.685	25000	1.705
Freundlich	A	0.988	-6.962	0.2858	0.066
	B	0.944	-13.208	3.3728	0.045
Temkin	A	0.971	-10.750	1.2853	0.071
	B	0.994	-10.834	1.3218	0.043

In general, when ΔG_{ads} is less than or equal to -20 kJ/mol, it is considered to be interactions between the charged molecules and the metal (physisorption), while those around -40 kJ/mol or higher are associated with chemisorption as a result of transfer or share of electrons from organic molecules to the metal surface to form a coordinate bond [36]. The calculated ΔG_{ads} values for inhibitors A and B are -37.374 and -35.685 kJ/mol for Langmuir; -6.962 and -13.208 kJ/mol for Freundlich; and -10.750 and -10.834 kJ/mol for Temkin respectively (Table 3). However, the best fit isotherm is Freundlich for inhibitor A and Temkin for inhibitor B. The calculated ΔG_{ads} for both inhibitors A and B are less than -20 kJ/mole in each case; therefore, the

adsorption mechanism of 5-methyl-2H-imidazol-4-carboxaldehyde (A) and 1H-Indole-3-carboxaldehyde (B) on mild steel in 1.0M HCl solution should be a typical physisorption.

3.5 Molecular descriptors for inhibitors A and B

The frontier molecular orbitals and Fukui functions for 5-methyl-2H-imidazol-4-carboxaldehyde (A) and 1H-Indole-3-carboxaldehyde (B) calculated using B3LYP/6-31+G** in aqueous medium were used to analyze the reactivity of the studied molecules. The highest occupied molecular orbital (HOMO) and the lowest unoccupied molecular orbital (LUMO) are related to the electron donating and accepting ability of a molecule respectively. Molecules with high HOMO energy (E_{HOMO}) would have high electrons donating tendency to acceptor spices with low LUMO energy (E_{LUMO}). Increase in HOMO energy increases binding ability of the inhibitor to the metal surface thereby facilitating adsorption, thus enhance the inhibition efficiency of the molecule [1]. The E_{HOMO}, E_{LUMO}, diploe moment, softness (S) and number of electrons transfer (Δn) for Inhibitor *A* are -7.82 eV, -2.93 eV, 1.35 Debye, 0.2342 and 0.166 respectively. In order to predict the preferred conformation of Inhibitor A in aqueous medium, calculations are performed on possible protonated structures (see Figure 1) of the inhibitor A at B3LYP/6-31+G** in aqueous medium. The E_{HOMO}, E_{LUMO}, diploe moment, softness (S) and number of electrons transfer (Δn) are -8.31 eV, -4.19 eV, 1.92 Debye, 0.2427 and 0.091 for protonation at N1; -7.98 eV, -3.48 eV, 8.11 Debye, 0.2222 and 0.141 for protonation at N2; and -8.74 eV, -4.86 eV, 8.36 Debye, 0.2577 and 0.0258 for di-protonations at N1, N2 respectively (Table 4). Therefore, higher E_{HOMO} value coupled with higher number of electron transfer in neutral inhibitor A would facilitate the flow of electrons from the lower electronegativity of the inhibitor A to the higher electronegativity iron surface (Table 4).

Table 4. Total Energy, Electron transfer, Softness and Hardness (A).

Molecular parameter	Neutral	Protonation at N1	Protonation at N2	Di-protonation at N1, N2
Total energy (au)	-378.870732	-379.297313	-379.308202	-379.723737
E_{HOMO} (eV)	-7.82	-8.31	-7.98	-8.74
E_{LUMO} (eV)	-2.93	-4.19	-3.48	-4.86
Dipole moment (Debye)	1.25	1.92	8.11	8.36
η	4.89	4.12	4.50	3.88
Softness	0.2045	0.2427	0.2222	0.2577
μ	-5.375	-6.250	-5.73	-6.80
Δn	0.166	0.091	0.141	0.0258
Dihedral angle				
C1-N1-C3-N4	0.00	0.00	0.00	0.00
N1-C1-N2-C4	0.00	0.00	0.00	0.00
N1-C3-C4-N2	0.00	0.00	0.00	0.00
N2-C2-N1-C3	0.00	0.00	0.00	0.00

Similarly, the E_{HOMO}, E_{LUMO}, diploe moment, softness (S) and number of electrons transfer (Δn) for Inhibitor B are also considered to guess the preferred conformation in aqueous medium. The E_{HOMO}, E_{LUMO}, diploe moment, softness (S) and Δn for inhibitor B are -6.29 eV, -1.81 eV, 6.27 Debye, 0.2232 and 0.329 respectively. For the protonations, the E_{HOMO}, E_{LUMO}, diploe moment, softness (S) and number of electrons transfer (Δn) are -6.99 eV, -2.83 eV, 8.60 Debye, 0.2404 and 0.251 for protonation at N (keto form); and -6.73 eV, -2.84 eV, 6.74 Debye, 0.2571 and 0.285 for protonation at N (enol form) respectively (Table 5). Higher E_{HOMO} and higher value of Δn for neutral inhibitor B would allow the flow of electrons from the lower electronegativity of the inhibitor to the higher electronegativity iron surface. However, presence of protonated forms of inhibitors A and B with lower E_{LUMO} in aqueous medium should increase the inhibitors ability to accept electron from d-orbital of iron until the chemical potential becomes equalized in aqueous medium [30, 33].

Table 5. Total Energy, Electron transfer, Softness and Hardness (B)

Molecular parameter	Neutral	Protonated at N (ketone form)	Protonated tautomer at N (enol form)
Total energy (au)	-477.179693	-477.577147	-477.607418
E_{HOMO} (eV)	-6.29	-6.99	-6.73
E_{LUMO} (eV)	-1.81	-2.83	-2.84
Dipole moment (Debye)	6.27	8.60	6.74
η	4.48	4.16	3.89
Softness	0.2232	0.2404	0.2571
μ	-4.05	-4.91	-4.785
Δn	0.329	0.251	0.285
Dihedral angle			
N-C3-C4-C5	0.00	0.00	0.00
C3-C4-C5-C1	0.00	0.00	0.00
C4-C5-C1-N	0.00	0.00	0.00
C5-C1-N-C3	0.00	0.00	0.00

Some of the important parameters (if other things being equal, because the nature of inhibitor interaction and efficiency may be dependent on the chemical, mechanical and structural characteristics of this layer) to measure reactivity of the inhibitor molecule towards the adsorption on the metallic surface are low energy band gap, high softness, high dipole moment and number of electrons transfer of the organic inhibitor. Comparison of calculated molecular parameters for inhibitors A and B reveal that inhibitor B presented lower energy band gap, ΔE ($\Delta E = E_{LUMO}–E_{HOMO}$); higher softness and higher dipole moment compared to inhibitor A. Decreasing in ΔE of the molecule has been attributed to increasing in the %IE of the molecule because lesser/lower energy would be required to remove an electron from the last occupied orbital [38]. Also, a molecule with a low energy gap is usually more polarisable with high chemical activity, low kinetic stability and high softness value [39, 40]; thus inhibitor B was expected to have higher % I.E as mentioned earlier. However, inhibitor A is observed experimentally with higher % I.E (%I.E = 62.96) compared to inhibitor B with %I.E of 51.50; the higher % I.E of inhibitor A may be due to: (1) presence of higher number of protonation sites as a result of higher number of nitrogen atoms [32], hence increase in number of electrostatic sites and (2) increase in number of planed protonated species

in addition to neutral specie (Tables 4 and 5) in aqueous medium as well as lower E_{LUMO} (E_{LUMO} = -2.93, -4.19, -3.48 and -4.86 eV for neutral, protonation at N1, protonation at N1 and di-protonations respectively) will facilitate higher ability of inhibitor A to accept electrons from d-orbital of iron than inhibitor B.

The Mulliken population charge analysis has been a useful parameter to estimate the adsorption centres of inhibitors. The Mulliken charges on N1 and N2 for inhibitor A -0.329 and -0.366*e* respectively. For inhibitor B, Mulliken charge on the only nitrogen atoms is -0.462*e*. It is generally agreed that the more negatively charged a heteroatom, the more it can be adsorbed on the metal surface [10] but presence of two nitrogen atoms in inhibitor A enhanced adsorption of inhibitor A on the metal surface. Another parameter that influenced higher % I.E of the inhibitor A is due to higher total electronic charges on ring atoms. The sum of Mulliken electronic charges on ring atoms are -1.858 and -0.858*e* for inhibitors A and B respectively which corresponded to the % I.E of the inhibitors [41].

Fukui functions which has been used to locate the local site for either electrophilic or nucleophilic attack on the molecules were calculated for the inhibitors using natural and Mulliken charges as shown in Tables 6 and 7. The f^- measures reactivity of an atom with respect to electrophilic attack (i.e. the characteristic of the molecule to donate electrons) and f^+ measures reactivity related to nucleophilic attack (i.e. the propensity of the molecule to accept electrons). The local reactivity for inhibitor A by mean of condensed Fukui functions shows that the most probable site for nucleophilic and electrophilic attack are on C1 and C2 respectively. Fukui functions calculated using natural and Mulliken electronic charges predicted the same nucleophilic and electrophilic centres for inhibitor A (Table 6). C8 and C9 are predicted for nucleophilic and electrophilic centres respectively for inhibitor B using natural electronic charges, however C5 is a, centre for both nucleophilic and electrophilic site using Mulliken electronic charges (Table 7).

Table 6. Fukui indices for nucleophilic and electrophilic sites on inhibitor A calculated using Natural and Mulliken electronic charges.

Natural Charges						Mulliken Charges				
atom	$qN_{(r)}$	$qN+1_{(r)}$	$qN-1_{(r)}$	f^+	f^-	$qN_{(r)}$	$qN+1_{(r)}$	$qN-1_{(r)}$	f^+	f^-
N1	-0.370	-0.588	-0.268	-0.218	-0.102	-0.329	-0.371	-0.237	-0.042	-0.092
N2	-0.451	-0.552	-0.319	-0.101	-0.132	-0.370	-0.366	-0.369	0.004	-0.001
C1	-0.174	-0.146	-0.183	**0.028**	0.009	-0.264	-0.290	-0.523	-0.026	**0.259**
C2	-0.728	-0.719	-0.741	0.009	**0.013**	-0.876	-0.478	-0.981	**0.398**	0.105
C3	0.078	-0.053	0.093	-0.131	-0.015	0.464	0.428	0.241	-0.036	0.223
C4	0.220	0.207	0.255	-0.013	-0.035	0.378	-0.050	0.678	-0.428	-0.300
C5	0.397	0.228	0.433	-0.169	-0.036	-0.052	-0.398	0.465	-0.346	-0.517
H1/H2	0.287	0.218	0.321	-0.069	-0.034	0.270	0.202	0.297	-0.068	-0.027
H4	0.192	0.131	0.364	-0.061	-0.172	0.245	0.151	0.419	-0.094	-0.174
H8	0.274	0.263	0.291	-0.011	-0.017	0.254	0.254	0.279	0.000	-0.025
H9	0.265	0.252	0.292	-0.013	-0.027	0.242	0.262	0.279	0.020	-0.037
H10	0.274	0.263	0.291	-0.011	-0.017	0.254	0.254	0.242	0.000	0.012
O	-0.552	-0.723	-0.146	-0.171	-0.406	-0.486	-0.599	-0.087	-0.113	-0.399

Table 7. Fukui indices for nucleophilic and electrophilic sites on inhibitor B calculated using Natural and Mulliken electronic charges.

Natural Charges						Mulliken Charges				
atom	$qN_{(r)}$	$qN+1_{(r)}$	$qN-1_{(r)}$	f^+	f^-	$qN_{(r)}$	$qN+1_{(r)}$	qN-1(r)	f^+	f^-
N	-0.538	-0.592	-0.461	-0.054	-0.077	-0.419	-0.462	-0.343	-0.043	-0.076
C1	0.066	-0.155	0.134	-0.221	-0.068	-0.028	-0.753	-0.055	-0.725	0.027
C2	0.389	0.119	0.384	-0.27	0.005	-0.524	-1.408	-0.611	-0.884	0.087
C3	0.128	0.122	0.126	-0.006	0.002	0.323	0.504	0.366	0.181	-0.043
C4	-0.083	-0.105	-0.084	-0.022	0.001	0.337	-0.108	0.583	-0.445	-0.246
C5	-0.267	-0.266	-0.697	**0.001**	**0.430**	0.393	0.078	0.700	-0.315	-0.307
C6	-0.257	-0.280	-0.128	-0.023	-0.129	-0.403	-0.345	-0.297	0.058	-0.106
C7	-0.245	-0.259	-0.135	-0.014	-0.110	0.014	0.813	-0.027	0.799	0.041
C8	-0.253	-0.28	-0.240	-0.027	-0.013	-0.378	0.622	-0.469	1.000	**0.091**
C9	-0.229	-0.245	-0.066	-0.016	-0.163	-0.697	0.793	-0.262	**1.490**	-0.435
H2	0.271	0.230	0.300	-0.041	-0.029	0.263	0.183	0.294	-0.08	-0.031
H3	0.473	0.448	0.498	-0.025	-0.025	0.507	0.497	0.527	-0.01	-0.020
H4	0.257	0.253	0.283	-0.004	-0.026	0.218	0.247	0.248	0.029	-0.030
H5	0.259	0.251	0.287	-0.008	-0.028	0.232	0.249	0.270	0.017	-0.038
H9	0.256	0.250	0.282	-0.006	-0.026	0.212	0.234	0.232	0.022	-0.020
H10	0.168	0.098	0.192	-0.070	-0.024	0.189	0.093	0.227	-0.096	-0.038

H14	0.251	0.241	0.279	-0.010	-0.028	0.202	0.186	0.253	-0.016	-0.051
O	-0.640	-0.829	-0.553	-0.189	-0.087	-0.638	-0.834	-0.637	-0.196	-0.001

4.0 CONCLUSION

- In the present study, the inhibition performance of 5-methyl-2H-imidazol-4-carboxaldehyde and 1H-Indole-3-carboxaldehyde on mild steel in 1.0MHCl was studied using weight-loss method and quantum chemical calculations.
- The inhibitor efficiency increased with the increase in inhibitor concentration. At highest concentrations, %IE of 5-methyl-2H-imidazol-4-carboxaldehyde was higher than that of 1H-Indole-3-carboxaldehyde.
- The adsorption of the two inhibitors showed that 5-methyl-2H-imidazol-4-carboxaldehyde and 1H-Indole-3-carboxaldehyde followed the Freundlich and Temkin isotherms respectively.
- The higher inhibition property of 5-methyl-2H-imidazol-4-carboxaldehyde could be related to the presence of higher number of protonation sites as a result of higher number of nitrogen atoms and increase in number of planed protonated species as well as and sum of the net charge of the ring atoms.

References

1. (a) P. Udhayakala, T.V. Rajendiran and S. Gunasekaran, J. of Adv. Sci. Res., 3(2), 37-44 (2012).
2. P. Udhayakala, T.V. Rajendiran and S. Gunasekaran, J. Comput. Methods Mol. Des., 2, 1-15 (2012).
3. M.K. Mwadham, C.M. Lutendo, O. Muzaffer, K. Faruk, D. Ilyas, I.B. Obot, and E.E. Eno, Int. J. Electrochem. Sci., 7, 5035 – 5056 (2012).
4. K.F. Khaled, Cor. Sci. 52, 3225-3234 (2010).
5. O. E. Nnabuk, I.I. Benedict, E. I. Nkechi, and E. E. Eno, Int. J. Electrochem. Sci., 6, 1027 – 1044 (2011).
6. C. Hui, F. Zhenghao, S. Wenyan, and X. Qi, Int. J. Electrochem. Sci., 7, 10121 - 10131 (2012).
7. I. Dehri and M. Ozcan, Mater. Chem and Phys., 98, 316 (2006).
8. M.G. Hosseini, M. Ehteshamzadeh, and T. Shahrabi, Electrochim Acta, 52, 3680 (2007).
9. M.M. El-Naggar, Corros. Sci., 49, 2226 (2007).
10. G. Zhang and C.B. Musgrave, Journal of Physical Chemistry A, 111(8), 1554–1561 (2007).
11. G. Bereket, E. Hur, and C. Ogretir, Journal of Molecular Structure: THEOCHEM, 578, 79–88 (2002).
12. J. Vosta and J. Eliasek, Corrosion Science, 11, 223–229 (1971).
13. E.E. Eno, A. Taner, K. Fatma, L. Ian, O. Cemil, S. Murat, and A.U. Saviour, Int. J. of Quantum Chem, 110, 2614–2636 (2010).
14. A.K. Dubey and G. Singh, Portugaliae Electrochimica Acta 25, 221-235 (2007).
15. N. Sally, L. Susana, N. Subramanya, and A. Ray, Mentzer M., 31, (2013).

16. I. Ahamad, R. Prasad, E.E. Ebenso and M.A. Quraishi, Int. J. of Electrochemica Sci, 7, 3436 – 3452 (2012).
17. V.S. Sastri, and J.R. Perumareddi, Corrosion science, 53, 617 (1997).
18. B. Semire and A.O. Odunola, Khimiya, 22(6), 893-906 (2013).
19. B. Gomez and N.V. Likhanova, J. Phys. Chem. B, 110, 8928 (2006).
20. I. Ahamad, R. Prasad, and M.A. Quraishi, Corros. Sci. 52, 933 (2010).
21. J. Fang, and J. Li, J. Mol. Struct. (Theochem), 593, 179 (2002).
22. N.O. Obi-Egbedi, K.E. Essien, I.B. Obot, E.E. Ebenso, Int. J. of Electrochemica Sci., 6, 913-930 (2012).
23. Spartan user's guide, Wave function, Inc, Irvine, CA 92612 USA
24. A.D. Becke, J. Chem. Phys. 98, 5648 (1993).
25. C. Lee, W.T. Yang, and R.G. Parr, Phys. Rev. B, 37, 785 (1988).
26. Z. Zhou and H.V. Navangul, J. Phys. Org. Chem., 3, 784-788 (1990).
27. T. Koopmans, Physica, 1, 104-113 (1934).
28. L. R. Domingo, M. Aurell, M. Contreras, and P. Perez, J. Phys. Chem. A., 106, 6871-6876 (2002).
29. W. Yang, and R. Parr, Proc. Nat. Acad. Sci. USA, 82, 6723–6726 (1985).
30. P. Udhayakala, A. Jayanthi, T.V. Rajendiran, Der Pharma Chemica, 3(6), 528-539 (2011).
31. E.E. Eno, A.I. David and O.E. Nnabuk, Int. J. Mol. Sci. 11, 2473-2498 (2010).
32. A. Singh, I. Ahamad, V.K. Singh, M.A. Quraishi, J. Solid State Electrochem. 15, 1087 (2011).
33. H.L. Wang, R.B. Liu, J. Xin, Corros Sci, , 46(10), 2455-2466 (2004).

34. A.Y. El-Etre, Mater. Chem. Phys. 108, 278 (2008).

34. S.P. Niketan, J. Smita and N.M. Girishkumar, Acta Chim. Slov. 57, 297–304 (2010).

35. J. Sutiana, A.A. Ahmed, K. Abdulhadi, H.K. Abdul Amir and M. Abu Bakar, int. J. Mol. Sci., 14(6), 11915-11928 (2013).

36. L. Pengju, F. Xia, T. Yongming, S. Chunning, and Y. Cheng, Mat. Sci. and App., 2, 1268-1278 (2011).

37. H.E El Sayed, E. Ahmed, A.E. Samy, and R. Safaa, General Papers ARKIVOC, (xi) 205-220 (2006).

38. I. Fleming, New York: John Wiley & Sons (1976).

39. A. Ghazoui, R. Saddik, N. Benchat, M. Guenbour, B. Hammouti, S.S. Al-Deyab and A. Zarrouk, Intern. J. Electrochem. Sci., 7,7080 – 7097 (2012).

40. I. Lukovits, E. Kalman and F. Zucchi, Corrosion Science, 57, 3-8 (2001).

41. K. Babic-Samardzija, K.F. Khaled and N. Hackerman, Anti-Corrosion Methods and Materials, 52(1), 11–21 (2005).